Electronic Supplementary Material (ESI) for Inorganic Chemistry Frontiers.

Supporting Information

Cr^{3+}-doped borate phosphors for broadband near-infrared LED applications

Jiutian Wang[a,b], Lihong Jiang*[a], Ran Pang[a], Su Zhang[a], Da Li[a], Kai Li[a], Chengyu Li*[a,b,c] and Hongjie Zhang[a,c,d]

[a] *State key Laboratory of Rare Earth Resource Utilization, Changchun Institute of Applied Chemistry, Chinese Academy of Sciences, Changchun 130022, P. R. China*

[b] *University of Science and Technology of China, Hefei 230026, China*

[c] *Zhongke Rare Earth (Changchun) Co., Ltd., Changchun 130000, P. R. China*

[d] *The GBA National Institute for Nanotechnology Innovation, Guangzhou, Guangdong 510535, P. R. China*

** Corresponding author: Tel: +86-0431-85262258*

E-mail address: cyli@ciac.ac.cn and lhjiang@ciac.ac.cn

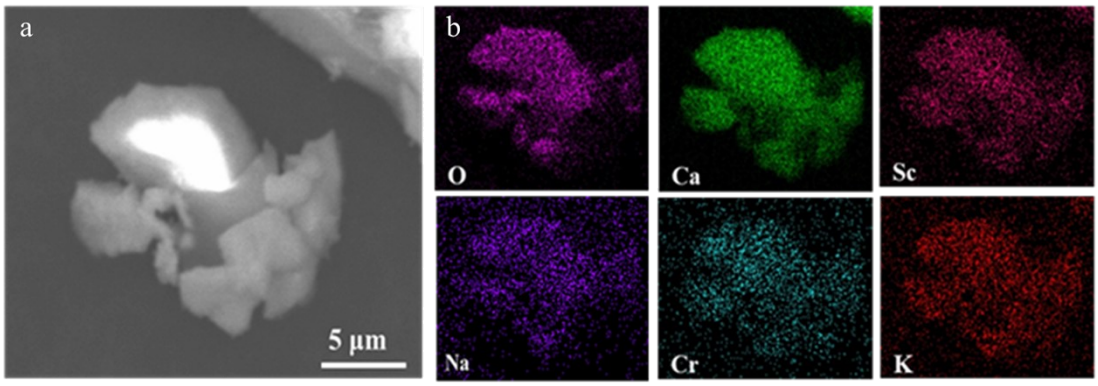

Fig. S1 (a) SEM images of KLNCSBO:0.02Cr^{3+}. (b) Elemental mapping of a representative particle of KLNCSBO:0.02Cr^{3+}.

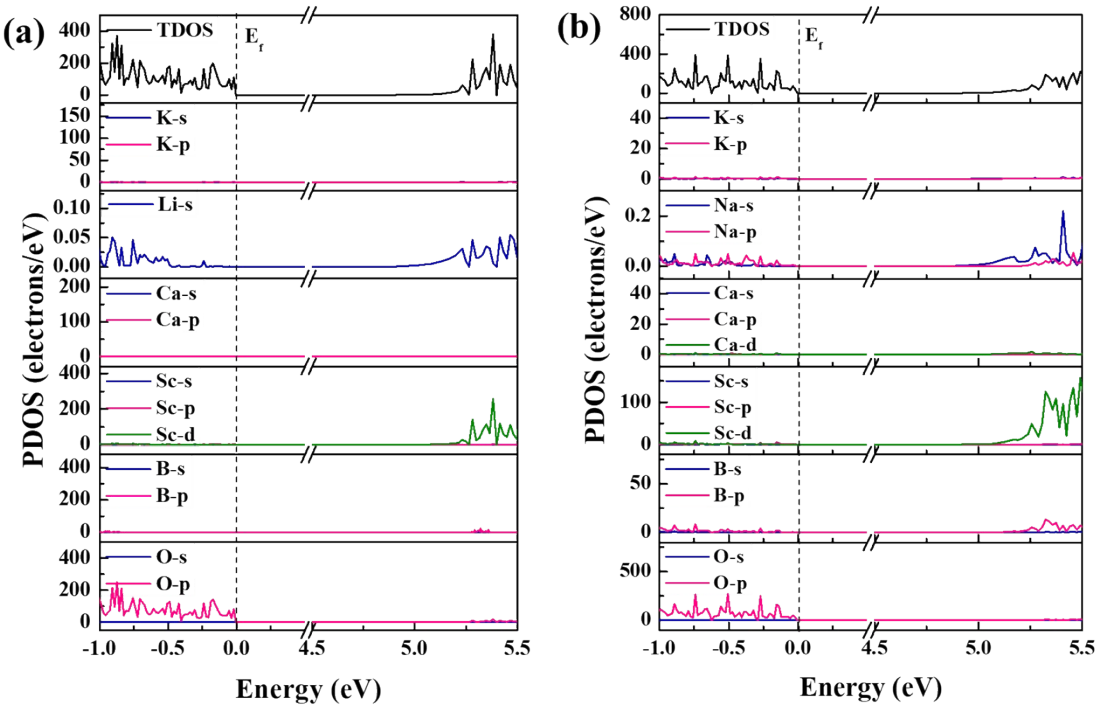

Fig. S2 (a) Local magnification PDOS of KLCSBO, (b) Local magnification PDOS of KNCSBO.

XRD results show that all the samples correspond well to the standard peaks, and no redundant heteropeak appeared, indicating that all the samples are pure phase (Fig. 8a). Besides, the range of 2θ from 27.7° to 29.5° is locally magnified to analyze the subtle structural changes, as shown in Fig. 8b. With the concentration of Na^+ ion (x) increased from 0 to 1, the (2 2 0) and (0 2 4) diffraction peaks gradually separated from 28.2° and 28.6° to 27.9° and 28.7°, respectively. According to Bragg's Law, 2θ is related to the interplanar spacing. It indicates that by increasing the proportion of Na atom from 0 (KLCSBO) to 1 (KNCSBO), the interplanar spacing will be increased for (2 2 0) plane from 3.1753 to 3.1905 Å and reduced for (0 2 4) plane from 3.1272 to 3.1076 Å.

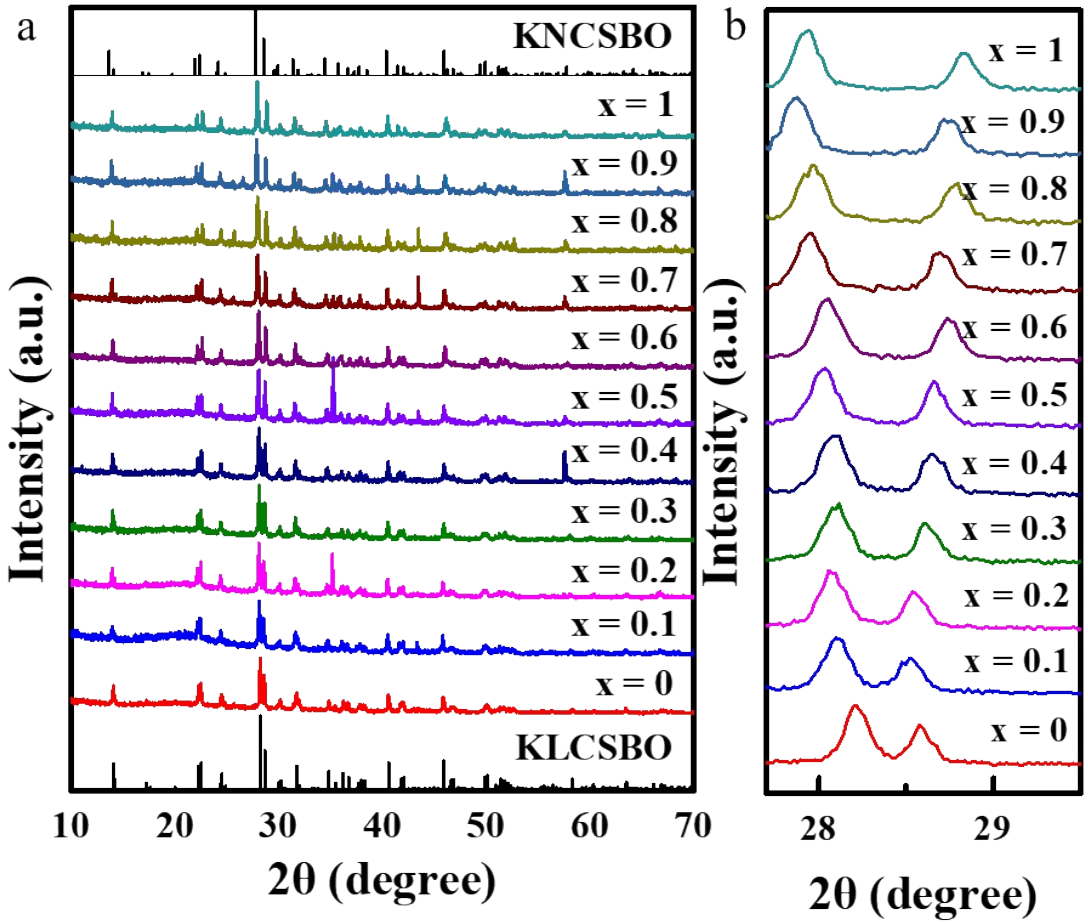

Fig. S3 (a) XRD patterns of $K_6Li_{1-x}Na_xCaSc_2(B_5O_{10})_3$:0.01$Cr^{3+}$ (x = 0-1) samples and the calculated XRD pattern of KLCSBO and KNCSBO. (b) Magnified XRD patterns from 28° to 29°.

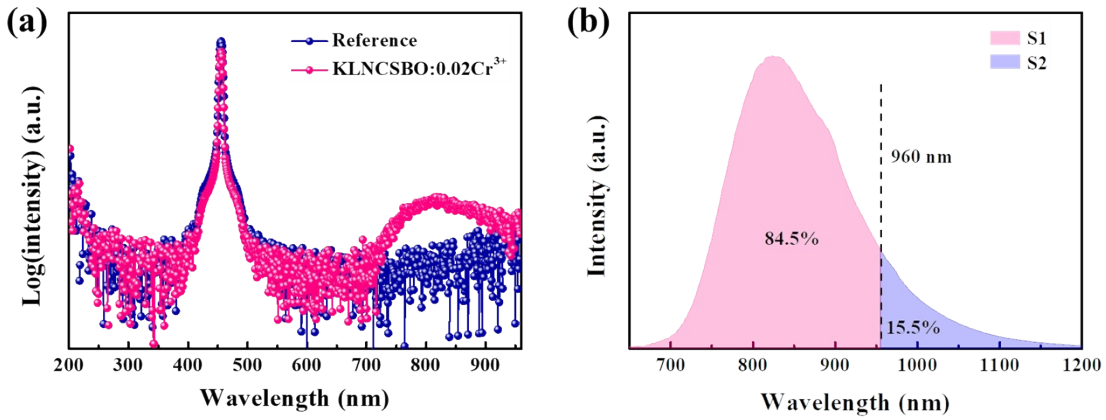

Fig. S4 (a) The spectra of the KLNCSBO:0.02Cr^{3+} phosphor and the reference sample (λ_{ex} = 456 nm) in quantum efficiency measurements. (b) The integral area of the PL emission spectrum of the KLNCSBO:0.02Cr^{3+} phosphor in the range of 650–960 nm and 960–1200 nm, respectively

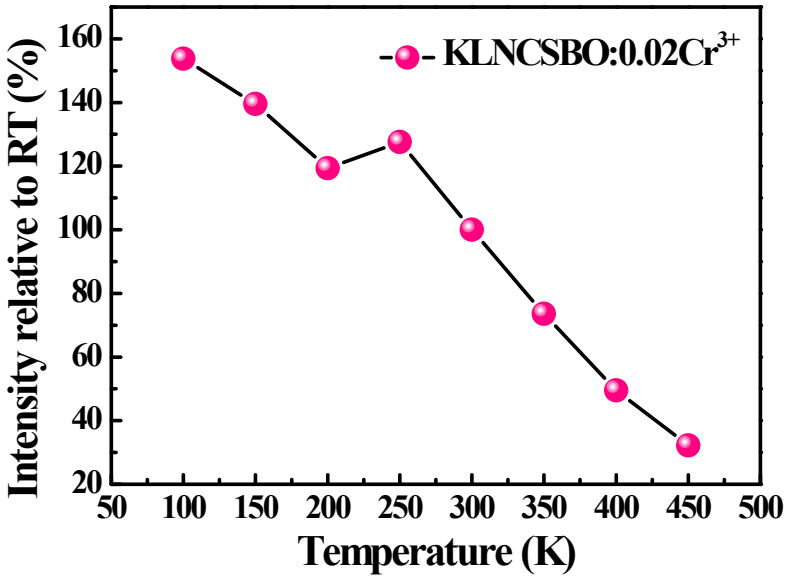

Fig. S5 The emission intensities of KLNCSBO:0.02Cr^{3+} versus temperature (λ_{ex} = 465 nm).

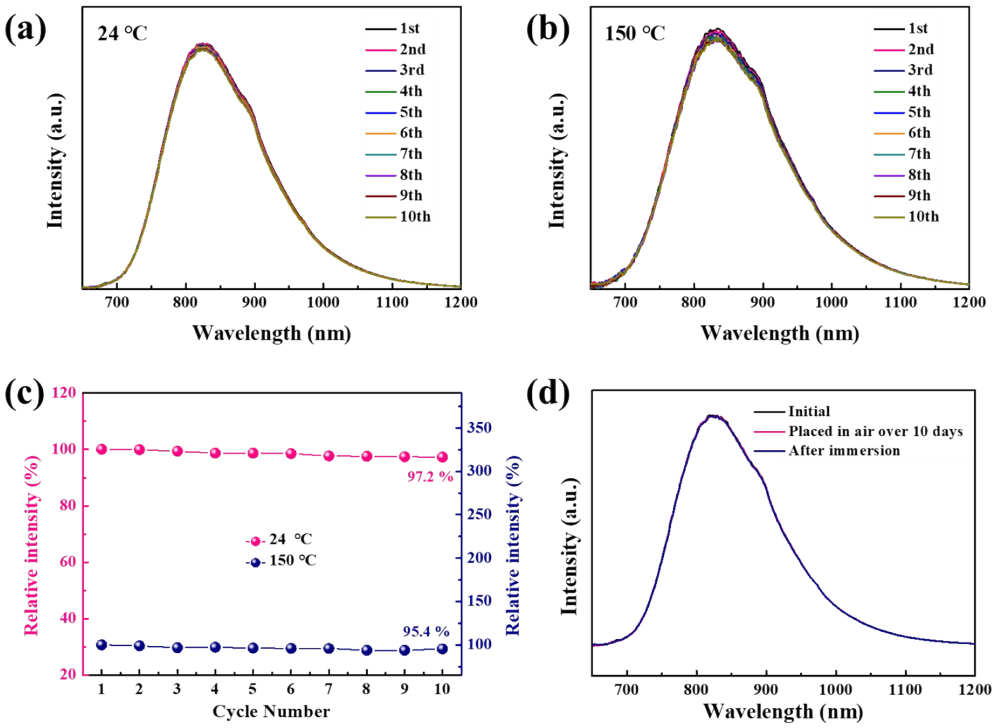

Fig. S6 (a) The PL spectra of KLNCSBO:0.02Cr^{3+} at 24 °C in 10 cycles (λ_{ex} = 465 nm), (b) The PL spectra of KLNCSBO:0.02Cr^{3+} at 150 °C in 10 cycles (λ_{ex} = 465 nm), (c) The relative emission intensity of KLNCSBO:0.02Cr^{3+} phosphor in 10 cycles, (d) The PL spectra of KLNCSBO:0.02Cr^{3+} under different conditions (λ_{ex} = 465 nm).

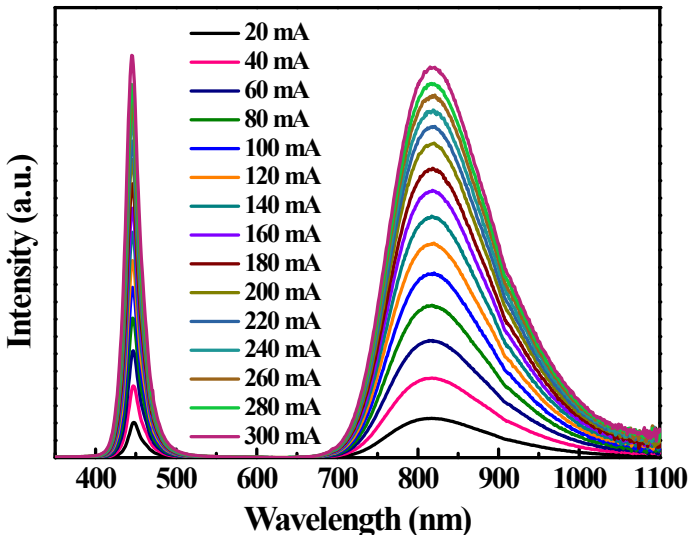

Fig. S7 (a) The EL spectra of KLNCSBO:0.02Cr^{3+} NIR pc-LED at various forward bias currents.

Table S1 Valences and effective ionic radius for related ions[1]

Ion	Valences	CN	IR (Å)
Cr^{3+}	3	6	0.615
Sc^{3+}	3	6	0.745
K^{+}	1	8	1.51
		10	1.59
Li^{+}	1	6	0.76
Na^{+}	1	6	1.02
Ca^{2+}	2	6	1.00
B^{3+}	3	3	0.01
		4	0.11

CN: Coordination number; IR: Effective ionic radius.

Table S2 Atomic positions of KLNCSBO

atom	x	y	z	Occupancy	U_{iso}
Li1	0.3333	0.6667	0.1667	1.000	0.0135
K1	0.2069	0.8735	0.3333	1.000	0.0095
K2	0.4947	0.4947	0.5	1.000	0.0096
Ca1	0.3333	0.6667	0.6667	1.000	0.0184
Sc1	0.3333	0.6667	0.4553	1.000	0.0145
B1	0.2169	0.4028	0.5579	1.000	0.0059
B2	0.218	0.218	0.5	1.000	0.0323
B3	0.1184	0.211	0.6438	1.000	0.0117
O1	0.2568	0.5213	0.5526	1.000	0.0120
O2	0.2321	0.3398	0.4893	1.000	0.0212
O3	0.157	0.336	0.6336	1.000	0.0012
O4	0.1536	0.144	0.423	1.000	0.0302
O5	0.059	0.1571	0.7171	1.000	0.0051

Table S3 Bond length of KLNCSBO (Å)

K1-O2	2.70553(8)	Ca1-O1	2.35956(6)
K1-O2	2.70464(8)	Ca1-O1	2.35907(6)
K1-O3	3.16245(7)	Ca1-O1	2.35981(6)
K1-O3	3.16233(7)	Ca1-O1	2.35905(6)
K1-O4	2.93093(6)	Averaged length	2.35968(93)
K1-O4	2.93051(6)	Sc1-O1	2.17852(5)
K1-O5	2.83193(6)	Sc1-O1	2.17855(5)
K1-O5	2.83227(6)	Sc1-O1	2.17773(5)
Averaged length	2.90758(1)	Sc1-O5	2.05741(4)
K2-O1(×2)	3.30220(7)	Sc1-O5	2.05756(4)
K2-O1(×2)	3.26436(7)	Sc1-O5	2.05841(4)
K2-O2(×2)	2.90854(6)	Averaged length	2.11803(45)
K2-O3(×2)	3.04383(12)	B1-O1	1.32911(3)
K2-O5(×2)	2.64213(6)	B1-O2	1.38618(3)
Averaged length	3.03221(74)	B1-O3	1.40690(4)
Li1/Na1-O4	2.22583(4)	Averaged length	1.37406(67)
Li1/Na1-O4	2.22524(4)	B2-O2(×2)	1.47487(3)
Li1/Na1-O4	2.22631(4)	B2-O4(×2)	1.46801(4)
Li1/Na1-O4	2.22522(4)	Averaged length	1.47144(35)
Li1/Na1-O4	2.22474(4)	B3-O3	1.41658(3)
Li1/Na1-O4	2.22582(4)	B3-O4	1.38091(3)
Averaged length	2.22553(07)	B3-O5	1.32786(4)
Ca1-O1	2.36029(6)	Averaged length	1.37512(0)
Ca1-O1	2.36032(6)		

Table S4 Bond length of KLNCSBO:0.06Cr^{3+} (Å)

K1-O2	2.70330(11)	Ca1-O1	2.35710(9)
K1-O2	2.70241(11)	Ca1-O1	2.35661(9)
K1-O3	3.15757(17)	Ca1-O1	2.35734(9)
K1-O3	3.15745(17)	Ca1-O1	2.35659(9)
K1-O4	2.92695(13)	Averaged length	2.35722(9)
K1-O4	2.92653(13)	Sc1/Cr1-O1	2.17608(8)
K1-O5	2.82769(14)	Sc1/Cr1-O1	2.17611(8)
K1-O5	2.82803(14)	Sc1/Cr1-O1	2.17529(8)
Averaged length	2.90374(26)	Sc1/Cr1-O5	2.05474(9)
K2-O1(×2)	3.29722(17)	Sc1/Cr1-O5	2.05489(9)
K2-O1(×2)	3.25944(17)	Sc1/Cr1-O5	2.05574(9)
K2-O2(×2)	2.90400(16)	Averaged length	2.11548(35)
K2-O3(×2)	3.04200(16)	B1-O1	1.32703(7)
K2-O5(×2)	2.63913(10)	B1-O2	1.38477(5)
Averaged length	3.02835(95)	B1-O3	1.40561(5)
Li1/Na1-O4	2.22294(9)	Averaged length	1.37247(57)
Li1/Na1-O4	2.22235(9)	B2-O2(×2)	1.47258(8)
Li1/Na1-O4	2.22342(9)	B2-O4(×2)	1.46661(6)
Li1/Na1-O4	2.22233(9)	Averaged length	1.46960(2)
Li1/Na1-O4	2.22185(9)	B3-O3	1.41438(8)
Li1/Na1-O4	2.22292(9)	B3-O4	1.37947(5)
Averaged length	2.22264(4)	B3-O5	1.32668(5)
Ca1-O1	2.35783(9)	Averaged length	1.37351(6)
Ca1-O1	2.35785(9)		

Table S5 Decay times of KLNCSBO:0.02Cr^{3+} under various temperatures

Temperature (K)	Decay time (μs)
100	68.14217
150	64.92274
200	59.69087
250	52.35736
300	43.06188
350	31.9606
400	21.59217
450	13.31018
500	7.58488

Table S6 Luminescent properties of KLNCSBO:0.02Cr^{3+} phosphor and some reported Cr^{3+}-doped broadband NIR phosphors in recent years

Host material	**Emission peak wavelength (nm)**	**FWHM (nm)**	**Emission intensity relative to RT**	**Ref.**
$K_6Li_{0.9}Na_{0.1}CaSc_2(B_5O_{10})_3$	825	167	49.5 % at 400 K	This work
$Ca_3Sc_2Si_3O_{12}$	770	93	85.6 % at 150 °C	[2]
$Y_2CaAl_4SiO_{12}$	744	160	78 % at 200 °C	[3]
$NaScGe_2O_6$	895	162	20.5 % at 150 °C	[4]
$Zn_3(Al_{1-x}Ga_x)_2Ge_2O_{10}$	721	70	–	[5]
$CaLu_2Mg_2Si_3O_{12}$	765	118.7	82.3 % at 423 K	[6]
$ScBO_3$	800	120	51 % at 150 °C	[7]
$Sr_8MgLa(PO_4)_7$	870	140	< 10 % at 400 K	[8]
$LiInSi_2O_6$	840	143	77 % at 150 °C	[9]

Table S7 The properties of NIR-LEDs prepared using KLNCSBO:0.02Cr^{3+} phosphor

Current (mA)	Voltage (V)	Input power (mW)	Output power (mW)
20	2.663	52.99	2.41
40	2.718	108.5	4.902
60	2.763	165.5	7.268
80	2.803	224	9.509
100	2.84	283.7	11.6
120	2.875	344.7	13.56
140	2.909	407	15.41
160	2.942	470.4	17.19
180	2.973	534.8	18.82
200	3.005	600.8	20.57
220	3.035	667.3	21.93
240	3.064	734.9	23.29
260	3.092	803.7	24.55
280	3.121	873.5	25.75
300	3.149	944.4	27.53

Reference

1. R. D. Shannon, Revised effective ionic radii and systematic studies of interatomie distances in halides and chaleogenides, *Acta Cryst.*, 1976, **32**, 751-767.
2. Z. W. Jia, C. X. Yuan, Y. F. Liu, X. J. Wang, P. Sun, L. Wang, H. C. Jiang and J. Jiang, Strategies to approach high performance in Cr^{3+}-doped phosphors for high-power NIR-LED light sources, *Light Sci. Appl.*, 2020, **9**, 2095-5545.
3. M. Q. Mao, T. L. Zhou, H. T. Zeng, L. Wang, F. Huang, X. Y. Tang and R. J. Xie, Broadband near-infrared (NIR) emission realized by the crystal-field engineering of $Y_{3-x}Ca_xAl_{5-x}SixO_{12}:Cr^{3+}$ (x=0-2.0) garnet phosphors, *J. Mater. Chem. C*, 2020, **8**, 1981-1988.
4. X. F. Zhou, W. Y. Geng, J. Y. Li, Y. C. Wang, J. Y. Ding and Y. H. Wang, An ultraviolet-visible and near-infrared responded broadband NIR phosphor and its NIR spectroscopy application, *Adv. Opt. Mater.*, 2020, **8**, 1902003.
5. T. Y. Gao, W. D. Zhuang, R. H. Liu, Y. H. Liu, X. X. Chen and Y. Xue, Design and control of the luminescence in Cr^{3+}-doped NIR phosphors via crystal field

engineering, *J. Alloys Compd.*, 2020, **848**, 156557.

6. R. Y. Li, Y. F. Liu, C. X. Yuan, G. Leniec, L. J. Miao, P. Sun, Z. H. Liu, Z. H. Luo, R. Dong and J. Jiang, Thermally stable $CaLu_2Mg_2Si_3O_{12}:Cr^{3+}$ phosphors for NIR LEDs, *Adv. Opt. Mater.*, 2021, **9**, 2100388.
7. Q. Y. Shao, H. Ding, L. Q. Yao, J. F. Xu, C. Liang and J. Q. Jiang, Photoluminescence properties of a $ScBO_3:Cr^{3+}$ phosphor and its applications for broadband near-infrared LEDs, *RSC Adv.*, 2018, **8**, 12035-12042.
8. B. Malysa, A. Meijerink and T. Justel, Temperature dependent photoluminescence of Cr^{3+} doped $Sr_8MgLa(PO_4)_7$, *Opt. Mater.*, 2018, **85**, 341-348.
9. X. X. Xu, Q. Y. Shao, L. Q. Yao, Y. Dong and J. Q. Jiang, Highly efficient and thermally stable Cr^{3+}-activated silicate phosphors for broadband near-infrared LED applications, *Chem. Eng. J.*, 2020, **383**, 123108.